

# New insights into Key Determinants for Adenosine 1 Receptor Antagonists Selectivity using Supervised Molecular Dynamics Simulations

Giovanni Bolcato <sup>1</sup>, Maicol Bissaro <sup>1</sup>, Giuseppe Deganutti <sup>1</sup>, Mattia Sturlese <sup>2</sup> and Stefano Moro <sup>2,\*</sup>

<sup>1</sup> Molecular Modeling Section (MMS), Department of Pharmaceutical and Pharmacological Sciences, University of Padova, via Marzolo 5, 35131 Padova, Italy

<sup>2</sup> School of Life Sciences, University of Essex, Wivenhoe Park, Colchester, CO4 3SQ, U.K

\* Correspondence: [stefano.moro@unipd.it](mailto:stefano.moro@unipd.it)

**Supplementary Information**

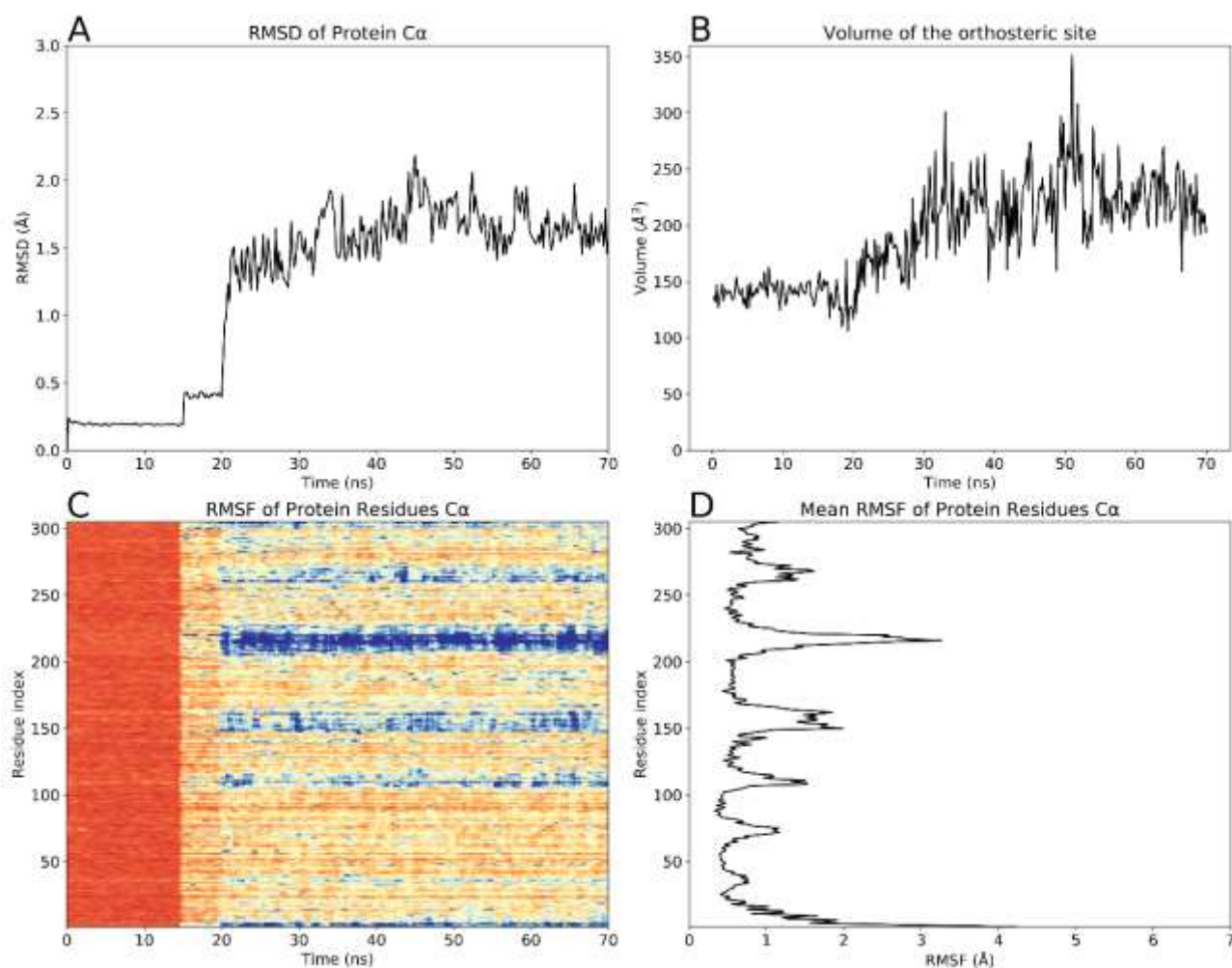


**Figure S1** A<sub>2A</sub>AR, protein analysis during the equilibration stage. Panel A: RMSD of the Protein Cα. Panel B: Volume of the orthosteric site. Panel C: RMSF of Protein residues Cα as a function of time, the RMSF value is plotted as a color, where blue indicates an higher value a red a lower value. Panel D: Mean RMSF of Protein residues Cα.

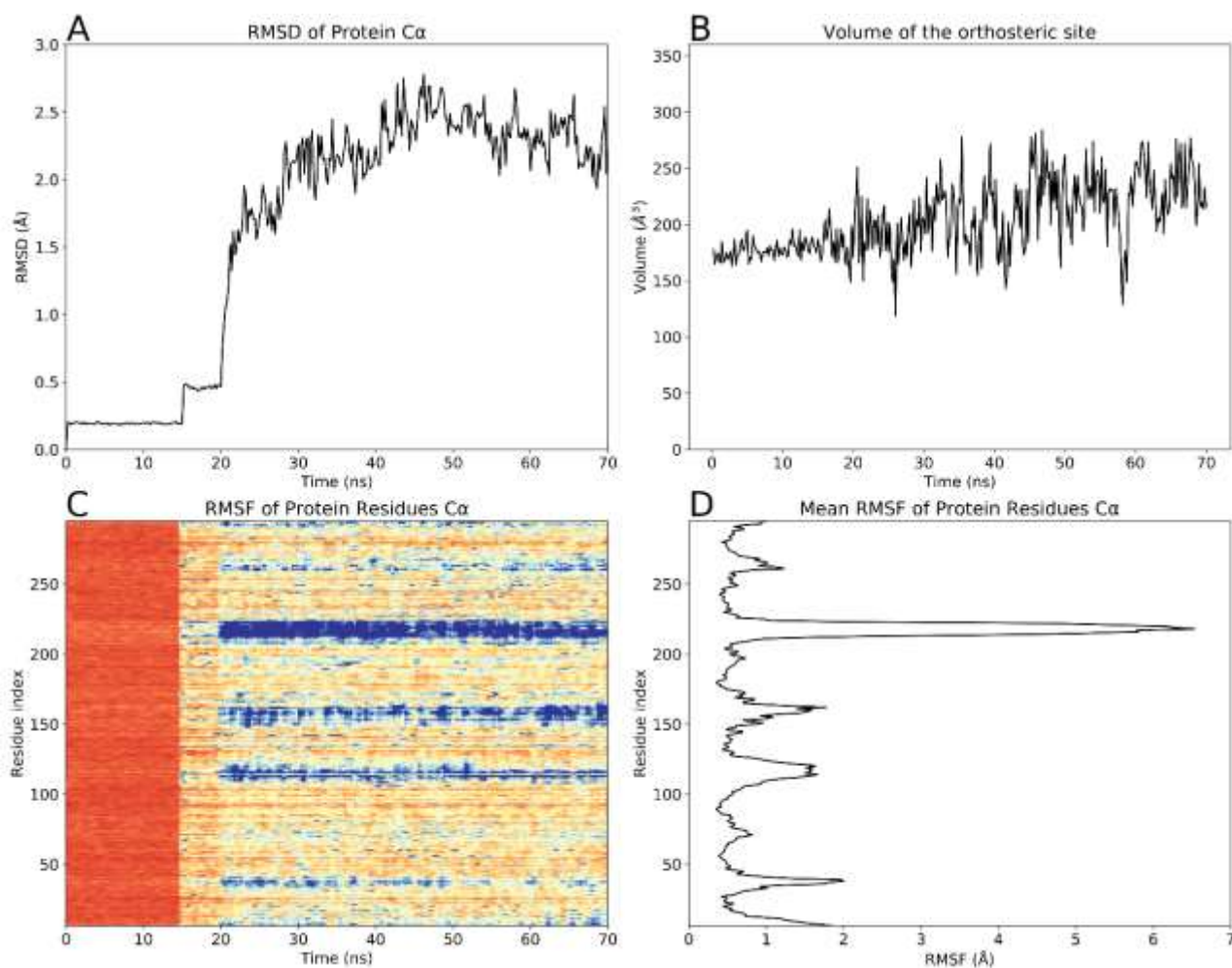


**Figure S2** A<sub>1</sub>AR, protein analysis during the equilibration stage. Panel A: RMSD of the Protein Cα. Panel B: Volume of the orthosteric site. Panel C: RMSF of Protein residues Cα as a function of time, the RMSF value is plotted as a color, where blue indicates an higher value a red a lower value. Panel D: Mean RMSF of Protein residues Cα.

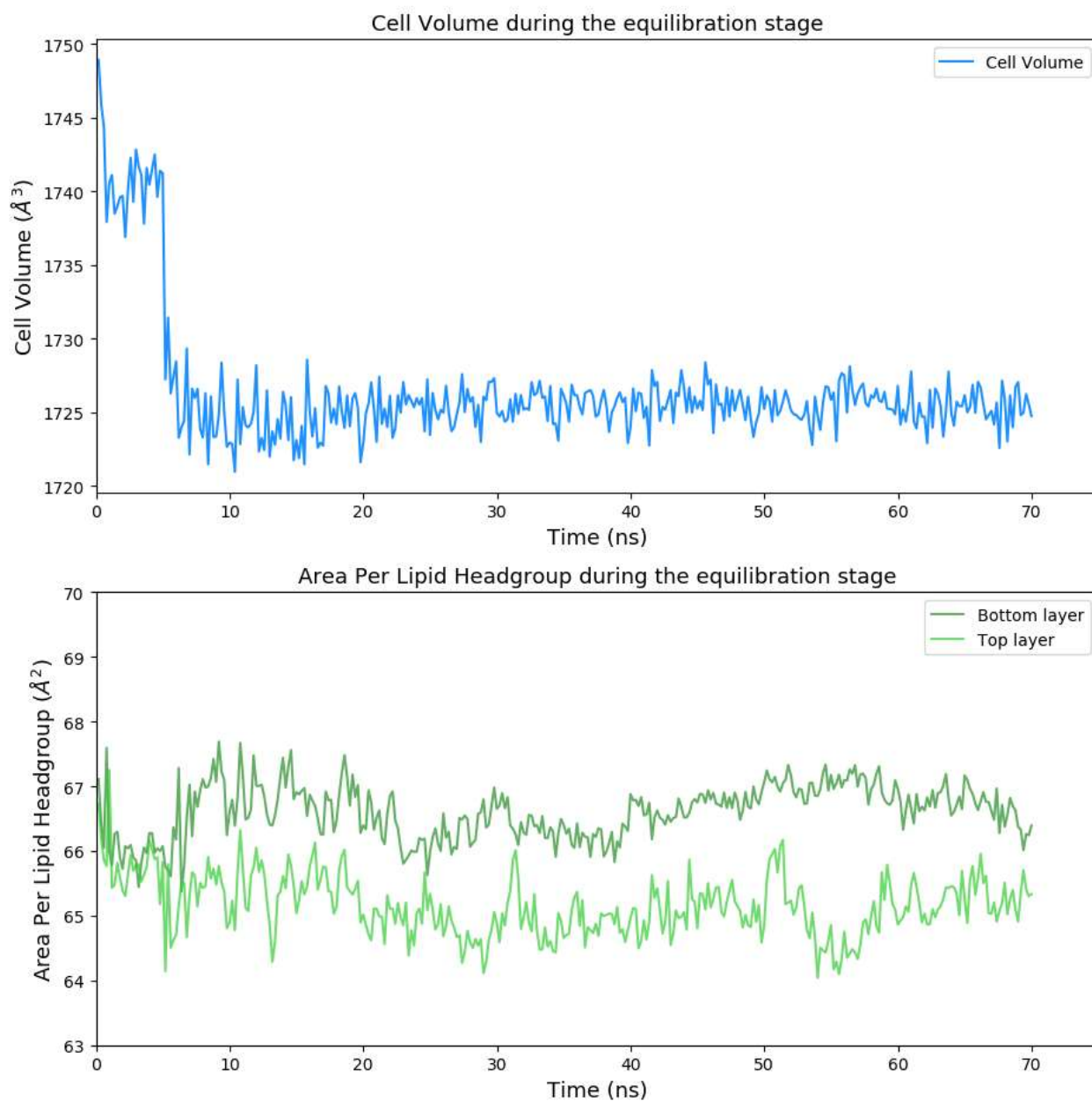


**Figure S3** A<sub>1</sub>AR system, cell volume analysis and membrane analysis. In the upper panel is reported the cell volume analysis. In the lower panel is reported the Area per Lipid Headgroup (analysis preformed with GRIDMAT).

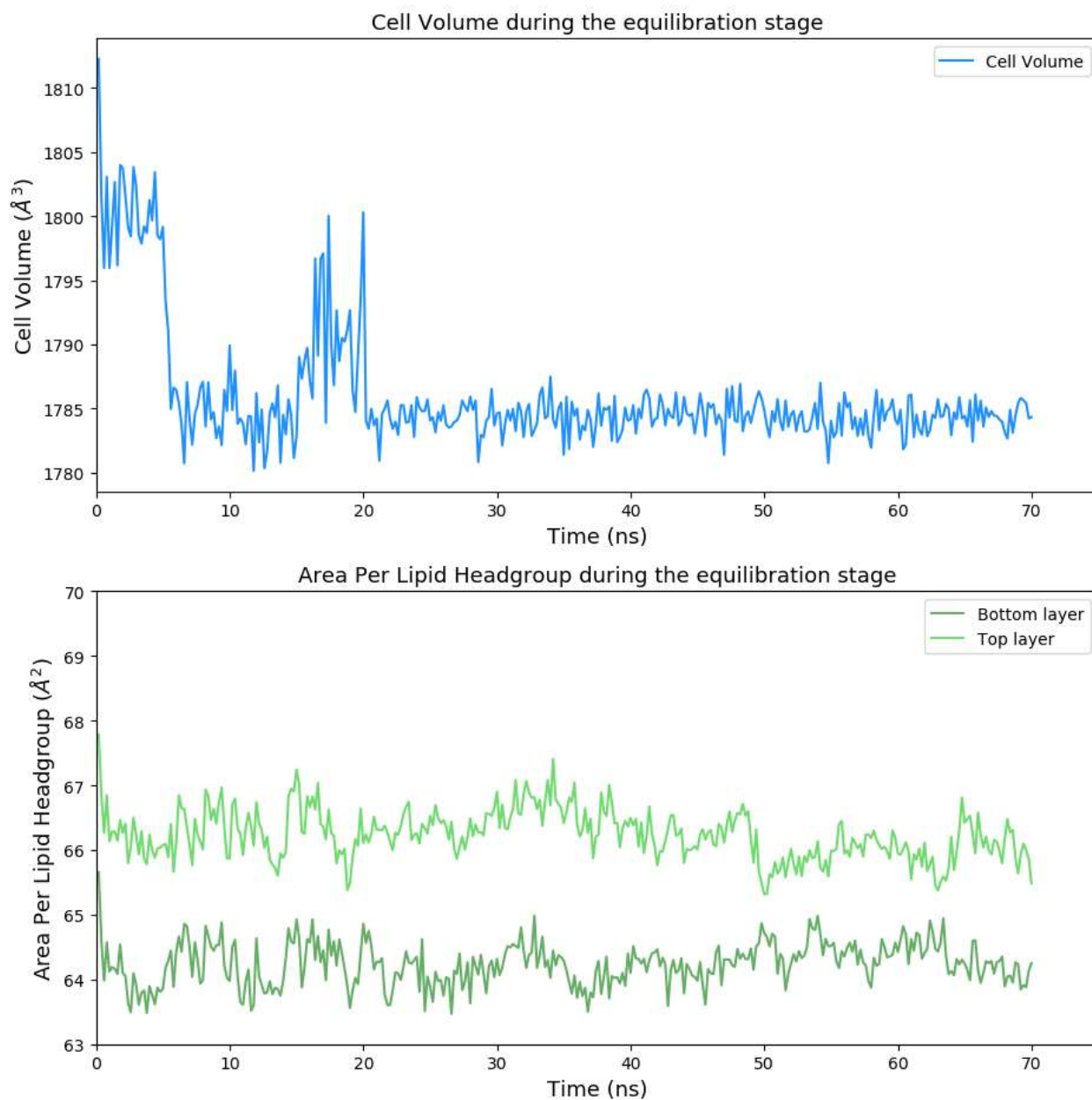


**Figure S4** A<sub>2A</sub>AR system, cell volume analysis and membrane analysis. In the upper panel is reported the cell volume analysis. In the lower panel is reported the Area per Lipid Headgroup (analysis performed with GRIDMAT).

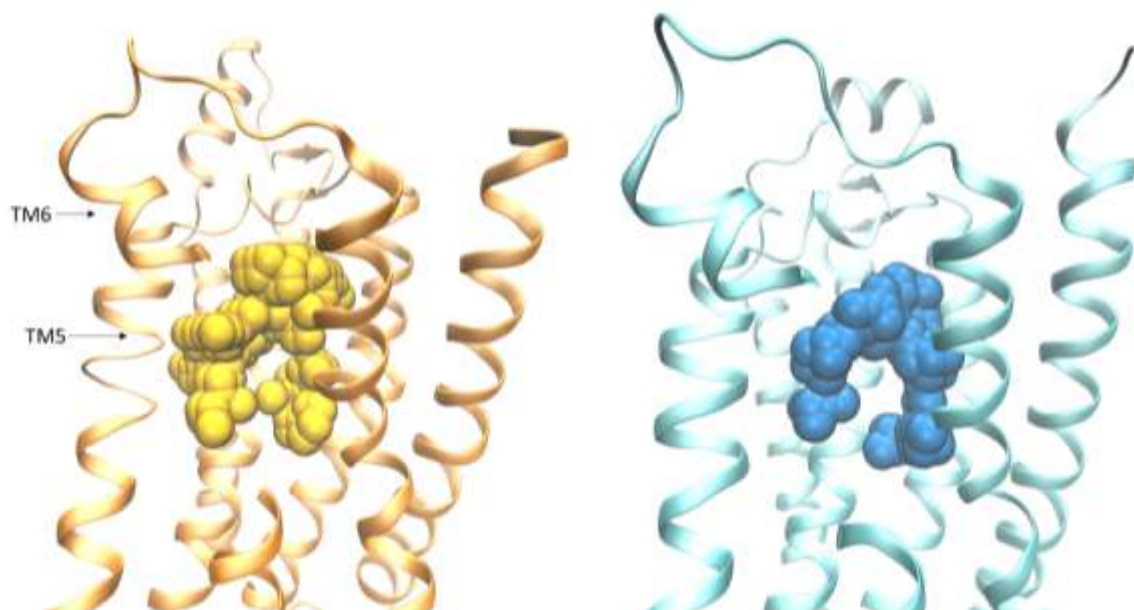


**Figure S5.** Volumetric analysis (using POVME) of the orthosteric site of A<sub>1</sub>AR and A<sub>2A</sub>AR. At the end of the equilibration stage, the orthosteric site of A<sub>1</sub>AR is deeper than the one of A<sub>2A</sub>-AR, especially between TM5 and TM6.



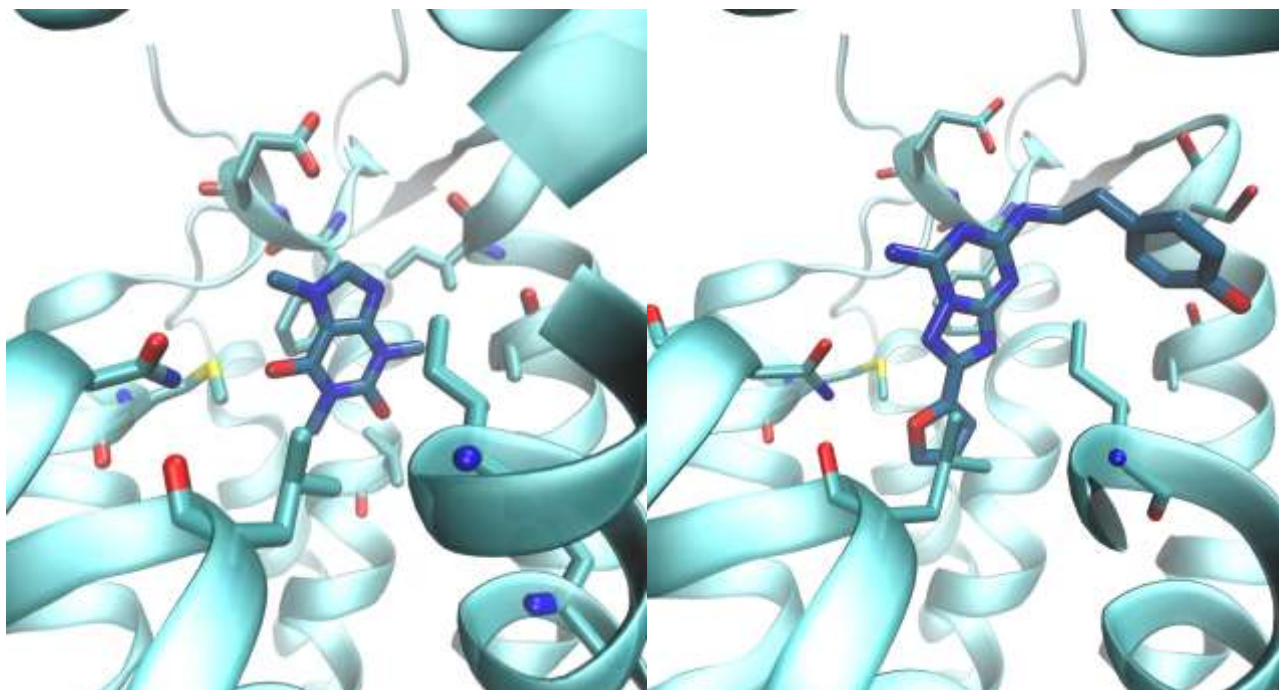


**Figure S6.** X-Ray structure of  $A_{2A}AR$  in complex with caffeine (left) and with ZMA (right)

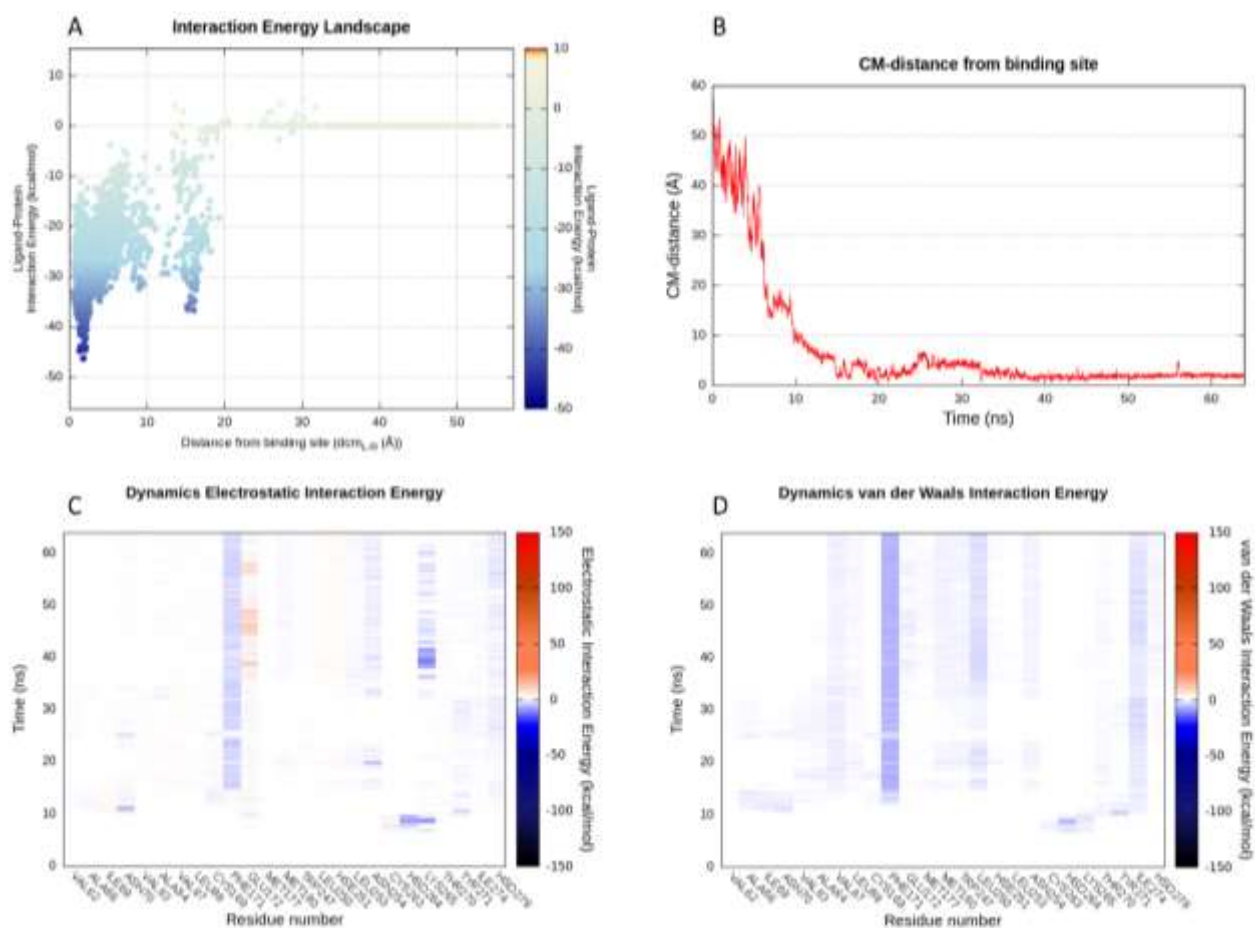


**Figure S7** Analysis of the SuMD trajectory of binding for caffeine on A<sub>1</sub>AR. Panel A: Ligand-protein interaction energy as a function of distance of the ligand from the binding site. Panel B: Distance between the center of mass of the ligand and the center of mass of the binding site over the time. Panel: Per-residue electrostatic interaction energy between ligand and protein. Panel D: Per residue van der Waals interaction energy between ligand and protein



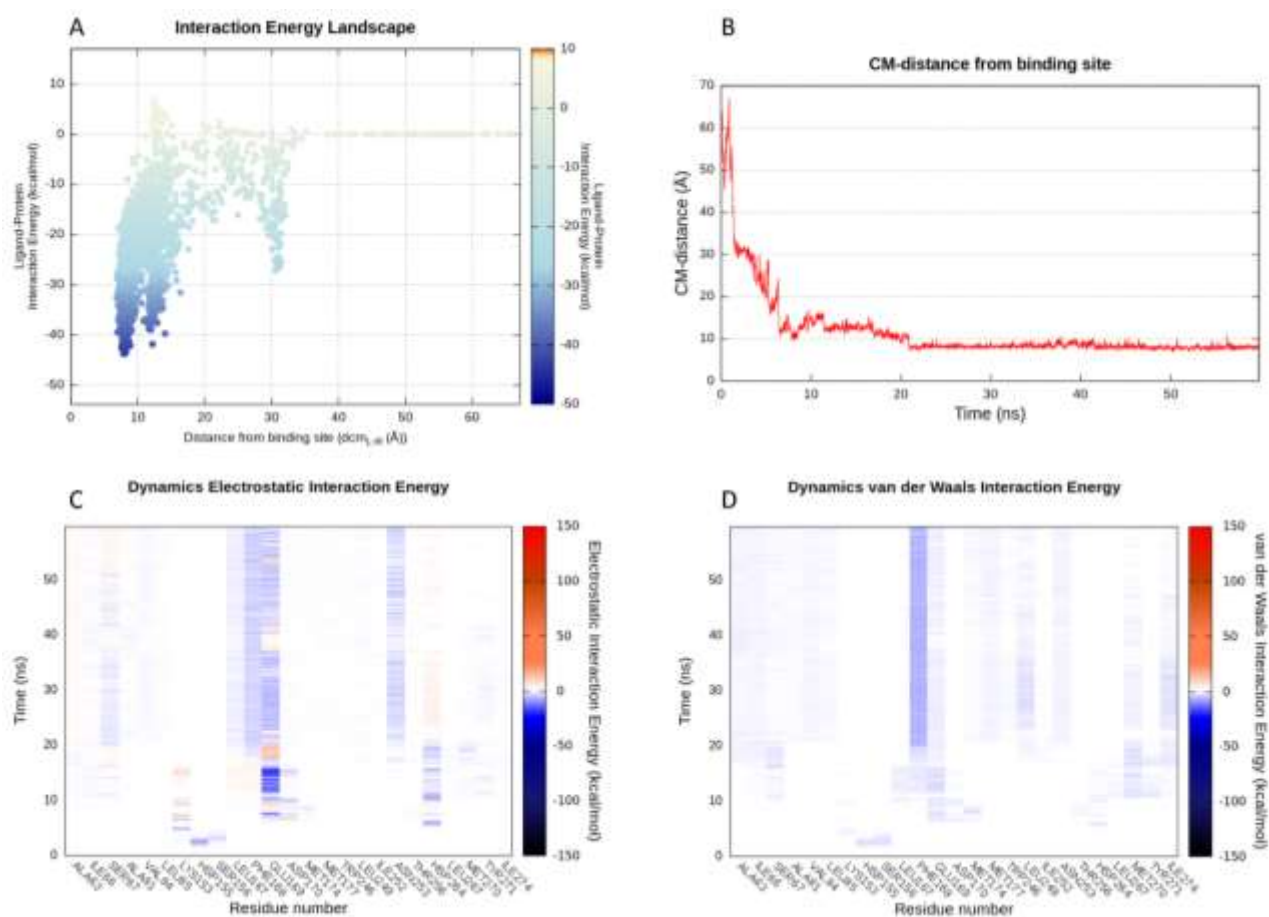


**Figure S8** Analysis of the SuMD trajectory of binding for caffeine on A<sub>2A</sub>AR. For a detailed explanation of each panel see Figure 5.

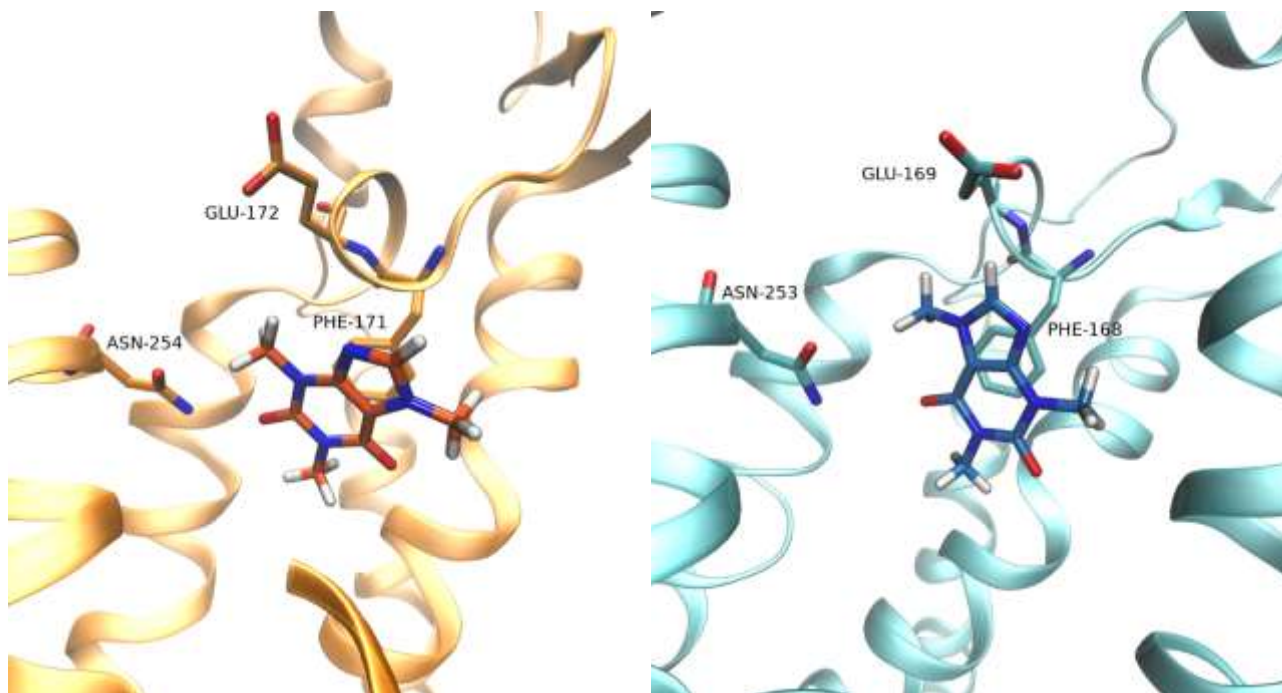


**Figure S9** Caffeine binding mode of caffeine within the binding site of A<sub>1</sub>AR, on the left-hand side, and within the A<sub>2A</sub>AR binding site, on the right-hand side.

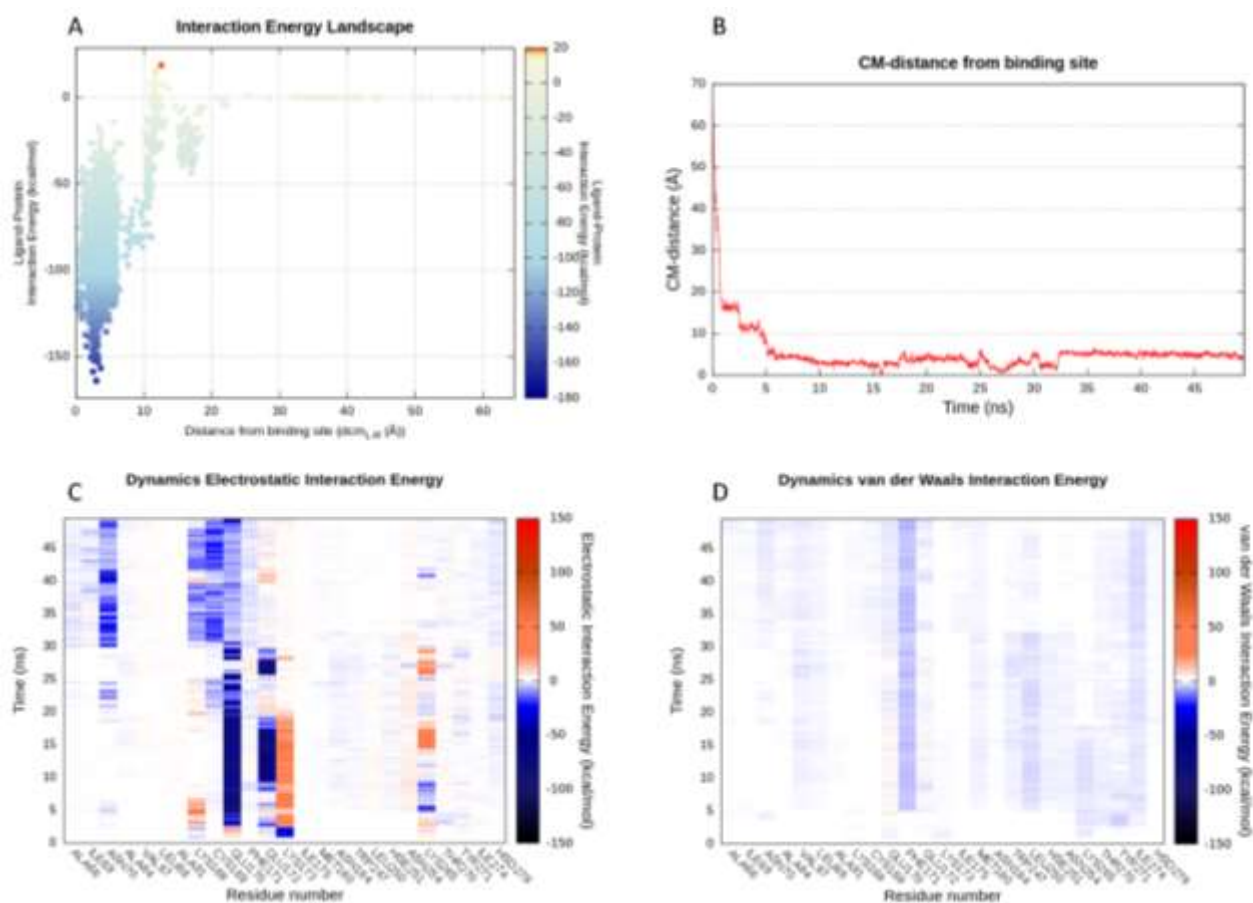


**Figure S10** Analysis of the Z48 SuMD binding trajectory to A<sub>1</sub>AR. For a detailed explanation of each panel see Figure S7

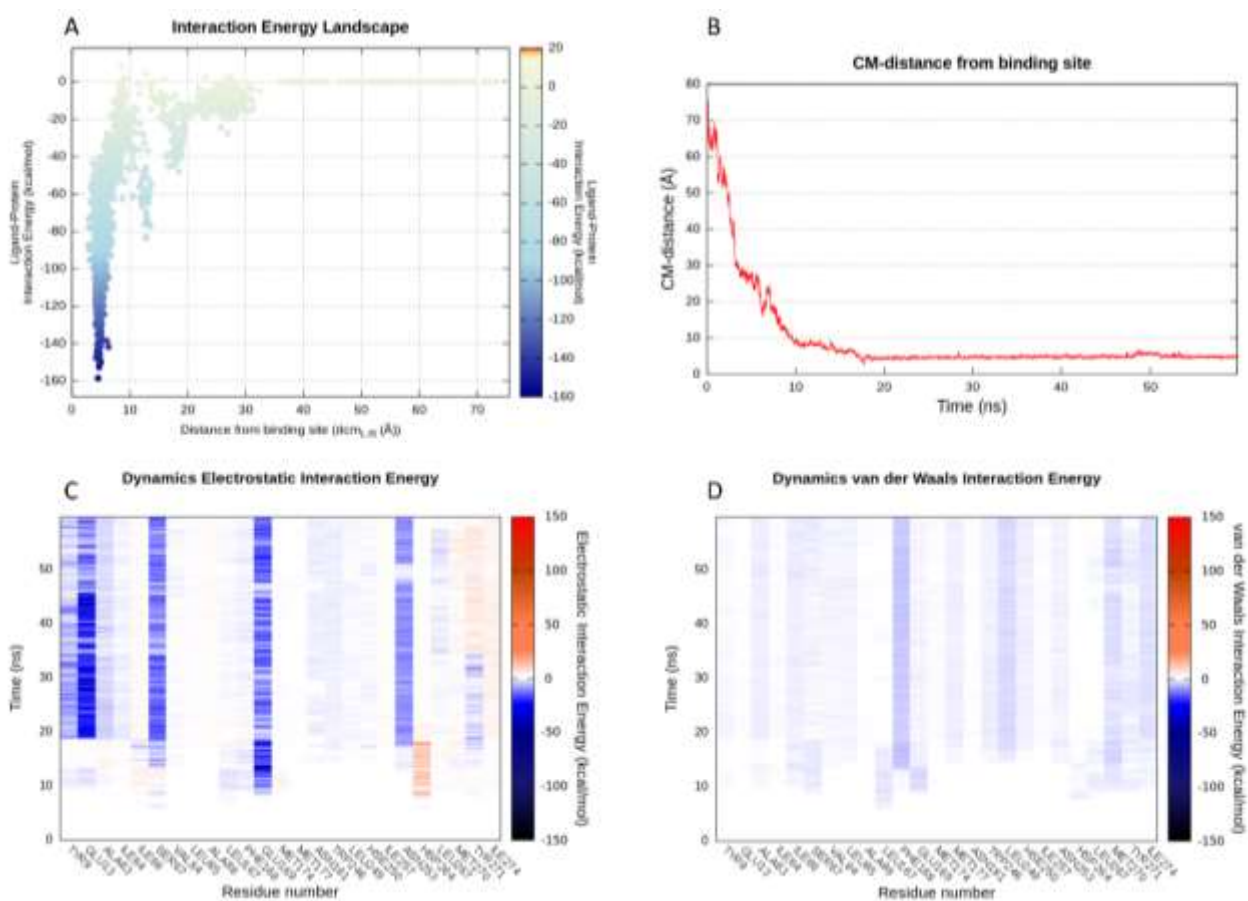


**Figure S11** Analysis of the SuMD trajectory of binding for Z48 on A<sub>2A</sub>AR. For a detailed explanation of each panel see Figure S7

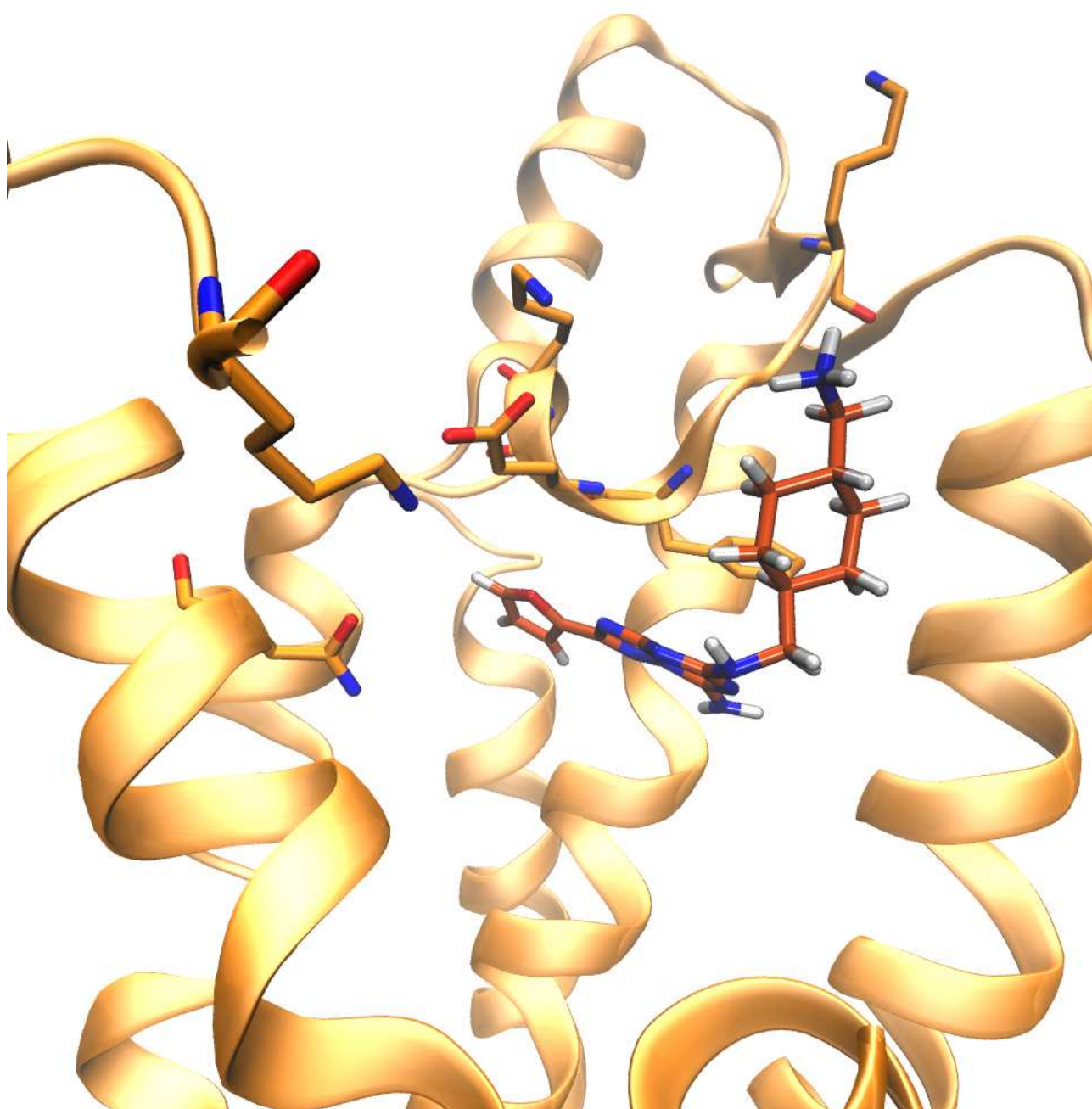


**Figure S12** Z48 in A<sub>1</sub>AR lose his binding mode in the 25 ns of classic MD performed at the end of SuMD.

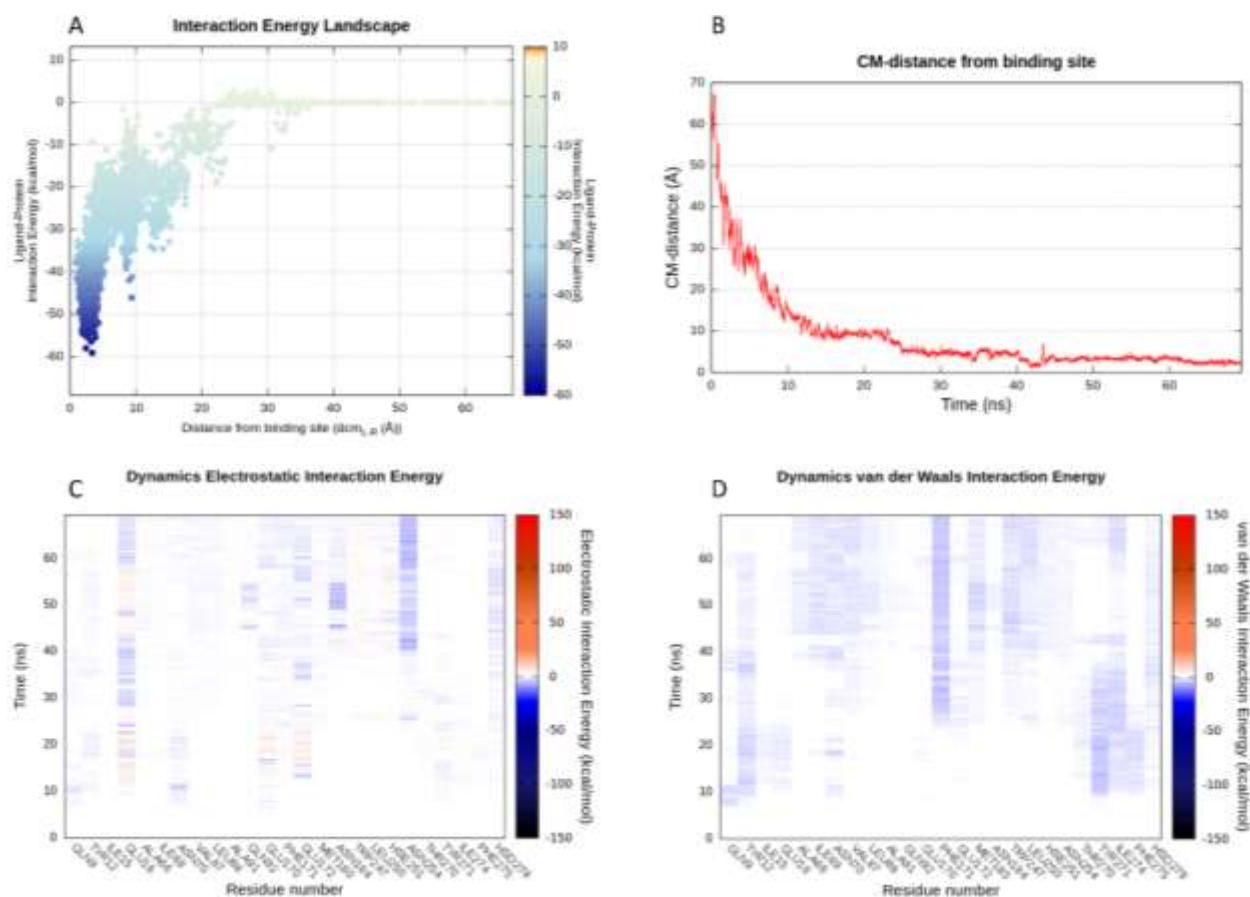


**Figure S13** Analysis of the SuMD trajectory of binding for LC4 on A<sub>1</sub>AR. For a detailed explanation of each panel see Figure S7.



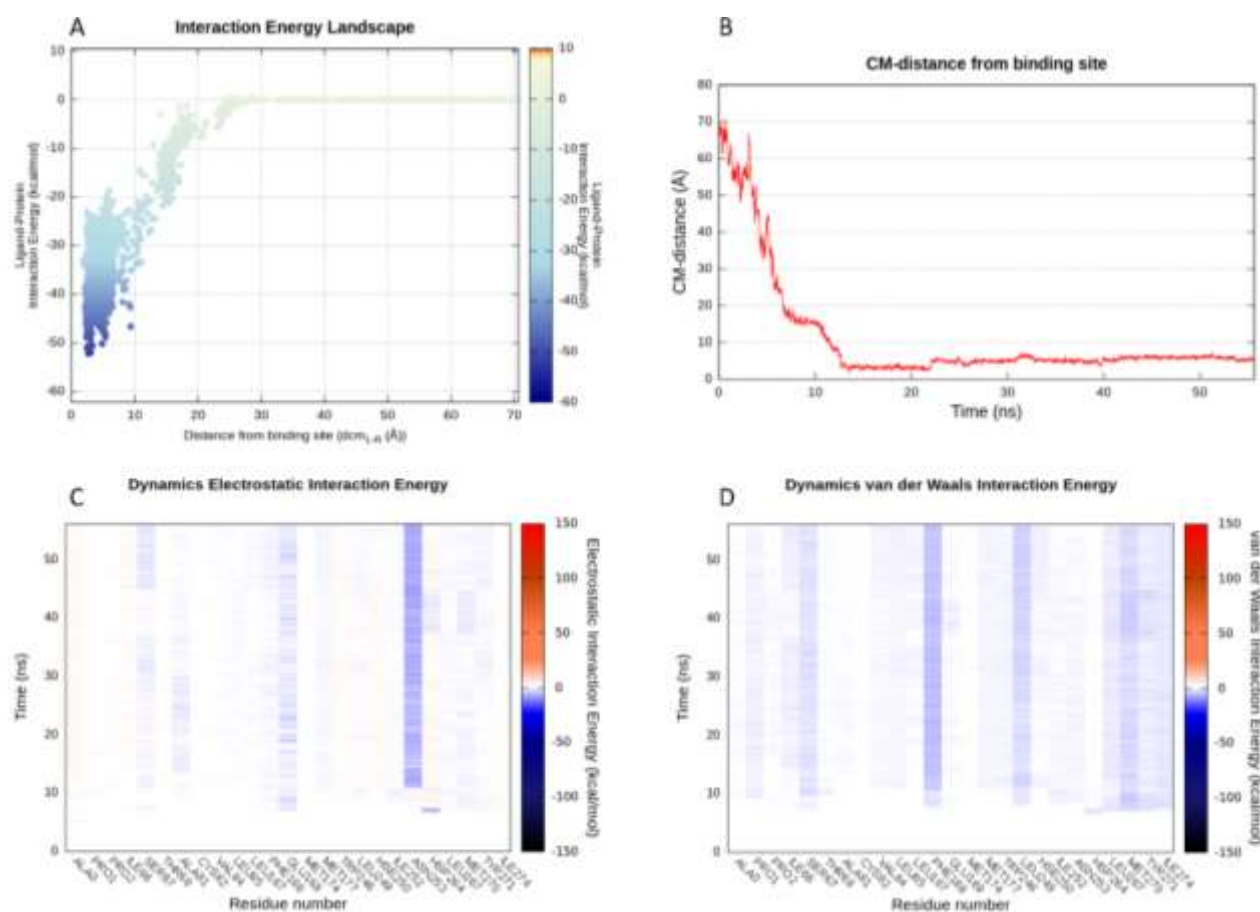


**Figure S14** Analysis of the SuMD trajectory of binding for LC4 on A<sub>2A</sub>AR. For a detailed explanation of each panel see Figure S7.

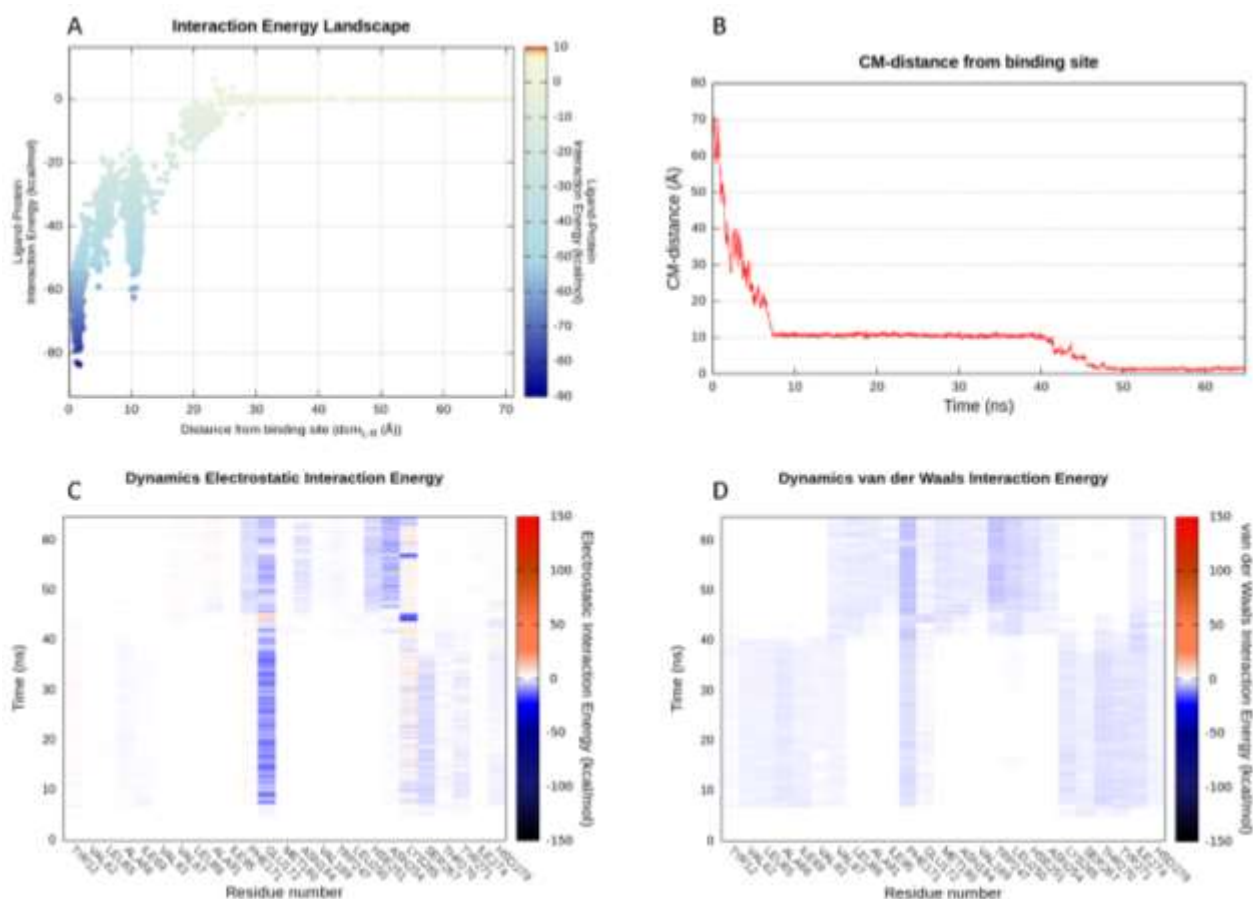


**Figure S15** Analysis of the SuMD trajectory of the alternative binding for LC4 on A<sub>1</sub>AR. As it can be seen in panel C and D, at the end the ligand adopts the classical binding mode interacting with ASN-254, GLU-172 and PHE-171.

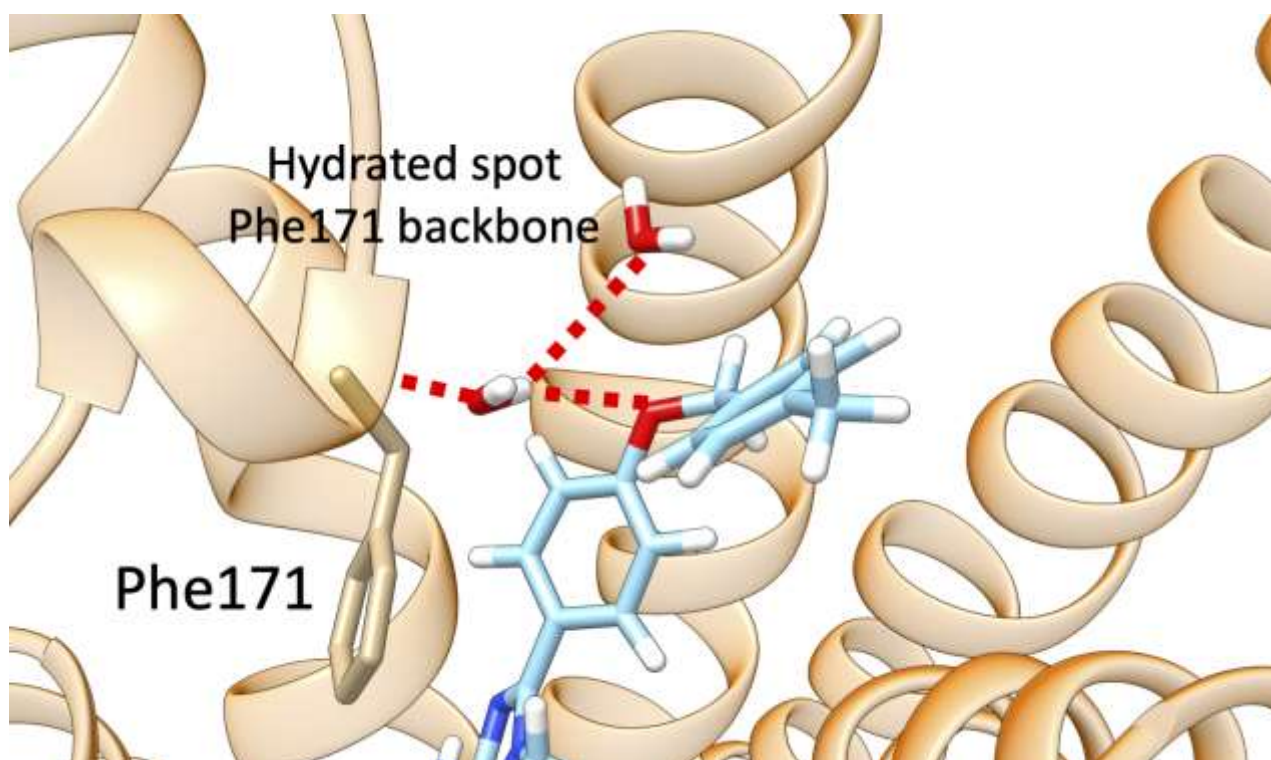


**Figure S16** The favorable intraction between LC4 and the water spot near the backbone of Phe171 in A<sub>1</sub>AR

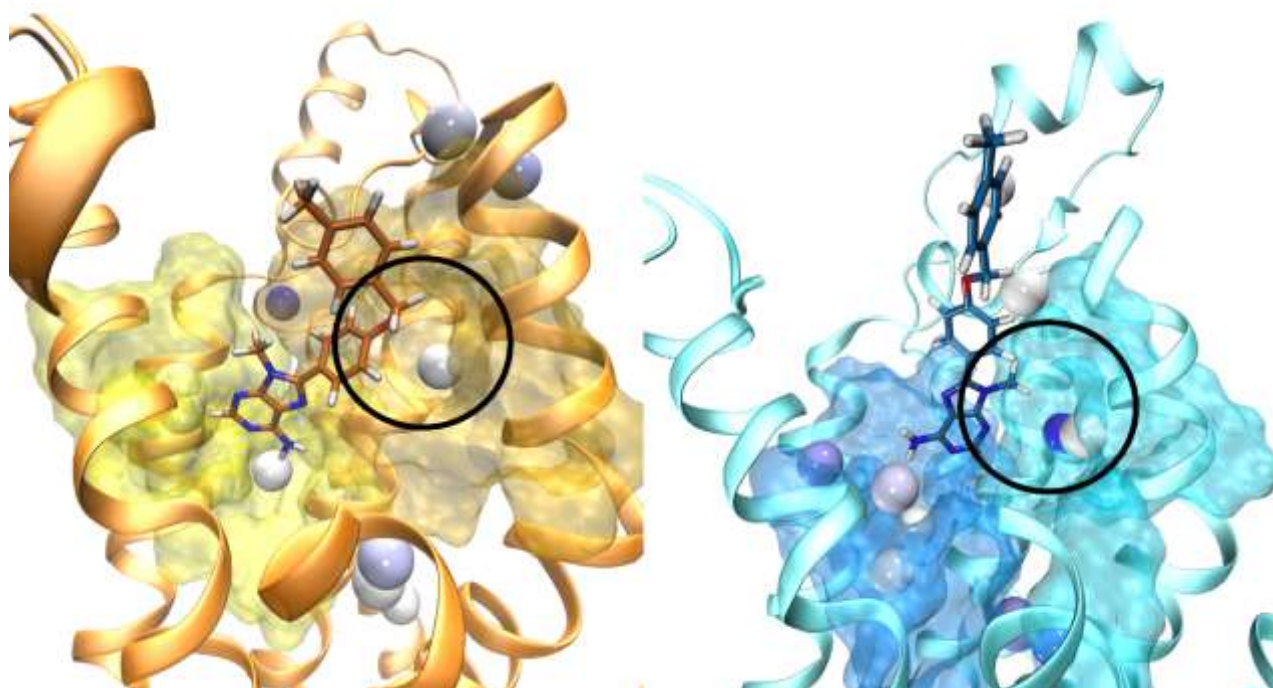


**Figure S17** LC4 within the binding site of A<sub>1</sub>-AR (on the left) and of on A<sub>2A</sub>-AR (on the right). In the first case the ligand interacts with the stationary water molecule in the hydrophobic pocket with an oxygen atom, while in the latter case with a methyl group.